PHYSICAL REVIEW D **88,** 114018 (2013)

Polarization effects in the cascade decay $\Lambda_b \to \Lambda(\to p\pi^-) + J/\psi(\to \ell^+\ell^-)$ in the covariant confined quark model

Thomas Gutsche,[1] Mikhail A. Ivanov,[2] Jürgen G. Körner,[3] Valery E. Lyubovitskij,[1,4] and Pietro Santorelli[5,6]

[1]*Institut für Theoretische Physik, Universität Tübingen, Kepler Center for Astro and Particle Physics, Auf der Morgenstelle 14, D-72076 Tübingen, Germany*

[2]*Bogoliubov Laboratory of Theoretical Physics, Joint Institute for Nuclear Research, 141980 Dubna, Russia*

[3]*PRISMA Cluster of Excellence, Institut für Physik, Johannes Gutenberg-Universität, D-55099 Mainz, Germany*

[4]*Department of Physics, Tomsk State University, 634050 Tomsk, Russia*

[5]*Dipartimento di Fisica, Università di Napoli Federico II, Complesso Universitario di Monte S. Angelo, Via Cintia, Edificio 6, 80126 Napoli, Italy*

[6]*Istituto Nazionale di Fisica Nucleare, Sezione di Napoli, 80126 Napoli, Italy*

(Received 1 October 2013; published 4 December 2013)

We calculate the invariant and helicity amplitudes for the nonleptonic decay $\Lambda_b \to \Lambda + J/\psi,\ \psi(2S)$ in the covariant confined quark model. We discuss joint angular decay distributions in the cascade decay $\Lambda_b \to \Lambda(\to p\pi^-) + J/\psi,\ \psi(2S)(\to \ell^+\ell^-)$ and calculate some of the asymmetry parameters that characterize the joint angular decay distribution. We confirm expectations from the naive quark model that the transitions into the $\lambda_\Lambda = 1/2$ helicity states of the daughter baryon Λ are strongly suppressed leading to a near maximal negative polarization of the Λ. For the same reason the azimuthal correlation between the two decay planes spanned by $(p\pi^-)$ and $(\ell^+\ell^-)$ is negligibly small. We provide form factor results for the whole accessible q^2 range. Our results are close to lattice results at minimum recoil and light-cone sum rule results at maximum recoil. A new feature of our analysis is that we include lepton mass effects in the calculation, which allows us to also describe the cascade decay $\Lambda_b \to \Lambda(\to p\pi^-) + \psi(2S)(\to \tau^+\tau^-)$.

DOI: 10.1103/PhysRevD.88.114018 PACS numbers: 12.39.Ki, 13.30.Eg, 14.20.Jn, 14.20.Mr

I. INTRODUCTION

Recently the LHCb Collaboration has performed an angular analysis of the decay $\Lambda_b \to \Lambda + J/\psi$ where the Λ_b's are produced in pp collisions at $\sqrt{s} = 7$ TeV at the LHC (CERN) [1]. They reported on the measurement of the relative magnitude of the helicity amplitudes in the decay $\Lambda_b \to \Lambda + J/\psi$ by a fit to several asymmetry parameters in the cascade decay distribution $\Lambda_b \to \Lambda(\to p\pi^-) + J/\psi(\to \ell^+\ell^-)$. In the fit they were also able to measure the transverse polarization of the Λ_b relative to the production plane. From a theoretical point of view the nonleptonic decay $\Lambda_b \to \Lambda + J/\psi$ is quite attractive in as much as the factorizable tree diagram is the only contribution to the decay; i.e. there are no W-exchange contributions [color compensation (C), exchange (E) and bow-tie (B) in the terminology of [2]] as e.g. in $\Lambda_b \to \Lambda + \rho^0$. There have been a number of theoretical quark model calculations for the decay $\Lambda_b \to \Lambda + J/\psi$ that are based on the factorization hypothesis [3–10]. The results of some of these calculations have been compared to the new experimental results by the LHCb Collaboration. We mention that the LHCb Collaboration has not given a result on the branching fraction $B(\Lambda_b \to \Lambda + J/\psi)$ for which the PDG quotes an average value of $(5.8 \pm 0.8) \times 10^{-4}$ [11]. The latter was deduced from the measurements by the CDF [12] and D0 Collaborations [13].

In this paper we present a detailed analysis of the decay process $\Lambda_b \to \Lambda + J/\psi$ in the framework of the covariant quark model proposed and developed in Refs. [14–25] for the study of mesons and baryons that are treated as bound states of their constituent quarks. Particle transitions are calculated from multiloop Feynman diagrams in which freely propagating constituent quark fields connect the different nonlocal particle-quark vertices. We mention that the covariant quark model has recently been also applied to exotic tetraquark states [26,27] and their decays. Quark confinement has been incorporated into the covariant quark model in an effective way [28–32] through an infrared regularization of the relevant quark-loop diagrams that removes quark thresholds in the loop diagrams (see details in Refs. [28–32]).

Our paper is structured as follows. In Sec. II, we review the phenomenological aspects of the decay $\Lambda_b \to \Lambda + V$ where $V = J/\psi$ or $\psi(2S)$. This includes a discussion of kinematics, matrix elements, and invariant and helicity amplitudes. In Sec. III we write down joint angular decay distributions for the cascade decay $\Lambda_b \to \Lambda(\to p\pi^-) + V(\to \ell^+\ell^-)$ where $V = J/\psi$ or $\psi(2S)$. We also define some pertinent decay asymmetry parameters that characterize the angular decay distributions. In Sec. IV we review the salient features of the covariant confined quark model and present our form factor results, which we compare with the results of other model calculations. In Sec. V we carefully discuss the heavy quark limit (HQL) of our $\Lambda_b \to \Lambda$ form factor expressions. In Sec. VI we present our numerical results on helicity amplitudes, on the rate and on the asymmetry parameters in the decay processes $\Lambda_b \to \Lambda + J/\psi$ and $\Lambda_b \to \Lambda + \psi(2S)$. We have included the

latter decay since it allows us to discuss nonzero lepton mass effects in the kinematically allowed decay $\Lambda_b \to \Lambda + \psi(2S)(\to \tau^+\tau^-)$. Finally, in Sec. VII, we summarize our results.

II. $\Lambda_b \to \Lambda + J/\psi$ DECAY: MATRIX ELEMENT AND OBSERVABLES

The effective Lagrangian [33] for the $b \to sc\bar{c}$ transition is given by

$$\mathcal{L}_{\rm eff} = \frac{G_F}{\sqrt{2}} V_{cb} V_{cs}^* \sum_{i=1}^{6} C_i Q_i, \tag{1}$$

where the Q_i are the set of effective four-quark flavor-changing $b \to s$ operators

$$\begin{aligned} Q_1 &= (\bar{c}^{a_1} O^\mu b^{a_2})(\bar{s}^{a_2} O_\mu c^{a_1}), \\ Q_4 &= (\bar{s}^{a_1} O^\mu b^{a_2})(\bar{c}^{a_2} O_\mu c^{a_1}), \\ Q_2 &= (\bar{c}^{a_1} O^\mu b^{a_1})(\bar{s}^{a_2} O_\mu c^{a_2}), \\ Q_5 &= (\bar{s}^{a_1} O^\mu b^{a_1})(\bar{c}^{a_2} \tilde{O}_\mu c^{a_2}), \\ Q_3 &= (\bar{s}^{a_1} O^\mu b^{a_1})(\bar{c}^{a_2} O_\mu c^{a_2}), \\ Q_6 &= (\bar{s}^{a_1} O^\mu b^{a_2})(\bar{c}^{a_2} \tilde{O}_\mu c^{a_1}), \end{aligned} \tag{2}$$

and where $V_{cb} = 0.0406$ and $V_{cs}^* = 0.974642$ are Cabibbo-Kabayashi-Maskawa (CKM) matrix elements; $O^\mu = \gamma^\mu(1-\gamma^5)$ and $\tilde{O}^\mu = \gamma^\mu(1+\gamma^5)$. The C_i are the set of Wilson coefficients [33]

$$\begin{aligned} &C_1 = -0.257, \qquad C_2 = 1.009, \qquad C_3 = -0.005, \\ &C_4 = -0.078, \qquad C_5 \simeq 0, \qquad C_6 = 0.001. \end{aligned} \tag{3}$$

The quark-level matrix element contributing to the $\Lambda_b \to \Lambda + J/\psi$ decay is given by

$$M(b \to sc\bar{c}) = \frac{G_F}{\sqrt{2}} C_{\rm eff} V_{cb} V_{cs}^* (\bar{s} O^\mu b)(\bar{c}\gamma_\mu c), \tag{4}$$

where

$$C_{\rm eff} = C_1 + C_3 + C_5 + \xi(C_2 + C_4 + C_6). \tag{5}$$

The color factor $\xi = 1/N_c$ will be set to zero such that we keep only the leading term in the $1/N_c$ expansion. The corresponding matrix elements of the exclusive transition $\Lambda_b \to \Lambda + V$ is defined by

$$\begin{aligned} &M(\Lambda_b \to \Lambda + V) \\ &\quad = \frac{G_F}{\sqrt{2}} V_{cb} V_{cs}^* C_{\rm eff} f_V M_V \langle \Lambda | \bar{s} O_\mu b | \Lambda_b \rangle \epsilon^{\dagger\mu}(\lambda_V), \end{aligned} \tag{6}$$

where M_V and f_V are the mass and leptonic decay constant of J/ψ or $\psi(2S)$. Note that the effective current $(\bar{s}O_\mu b)$ appearing in the set of operators in Eq. (2) is left chiral. In the naive quark model where the spin of the Λ_b and the Λ are carried by the b and s quarks, respectively, one would conclude that the Λ is left chiral and therefore emerges with a dominant helicity of $\lambda_\Lambda = -1/2$. The dominance of the $\lambda_\Lambda = -1/2$ helicity configuration predicted in the naive quark model is borne out by our exact calculation.

The hadronic matrix element $\langle \Lambda | \bar{s} O_\mu b | \Lambda_b \rangle$ in (6) is expanded in terms of dimensionless invariant form factors f_i^J ($i = 1, 2, 3$ and $J = V, A$), viz.

$$\begin{aligned} \langle B_2 | \bar{s}\gamma^\mu b | B_1 \rangle &= \bar{u}_2(p_2)[f_1^V(q^2)\gamma^\mu - f_2^V(q^2) i\sigma^{\mu q}/M_1 \\ &\quad + f_3^V(q^2) q^\mu/M_1] u_1(p_1), \\ \langle B_2 | \bar{s}\gamma^\mu\gamma^5 b | B_1 \rangle &= \bar{u}_2(p_2)[f_1^A(q^2)\gamma^\mu - f_2^A(q^2) i\sigma^{\mu q}/M_1 \\ &\quad + f_3^A(q^2) q^\mu/M_1]\gamma^5 u_1(p_1), \end{aligned} \tag{7}$$

where $q = p_1 - p_2$. We have kept the scalar form factors f_3^V and f_3^A in the form factor expansion Eq. (7) although they do not contribute to the decay $\Lambda_b \to \Lambda + J/\psi$ since $q_\mu \epsilon_V^\mu = 0$. The reason is that we want to compare our results on the scalar form factor with the results of other model calculations. The scalar form factors would e.g. contribute to the rare decays $\Lambda_b \to \Lambda + \ell^+\ell^-$ and the decays $\Lambda_b \to \Lambda + \eta_c$ and $\Lambda_b \to p + \pi^-$. The relevant form factors have been calculated before by us in the covariant confined quark model [32]. We shall use the results of [32], but we will add a few explanatory remarks concerning the cascade decay process $\Lambda_b \to \Lambda(\to p\pi^-) + V(\to \ell^+\ell^-)$. We shall also present a detailed discussion of the HQL of our form factor expressions, which was not included in [32].

As is well known it is convenient to analyze the decay in terms of helicity amplitudes $H_{\lambda_2\lambda_V}$ that are linearly related to the invariant form factors f_i^V and f_i^A (see details in Refs. [24,25,32,34]). Here we shall employ a generic notation such that the parent and daughter baryons are denoted by B_1 and B_2. The helicities of the daughter baryon B_2 and the vector charmonium state V are denoted by λ_2 and λ_V. The pertinent relation is

$$\begin{aligned} H_{\lambda_2\lambda_V} &= \langle \Lambda(\lambda_2) | \bar{s} O_\mu b | \Lambda_b(\lambda_1) \rangle \epsilon^{\dagger\mu}(\lambda_V) \\ &= H^V_{\lambda_2\lambda_V} - H^A_{\lambda_2\lambda_V}. \end{aligned} \tag{8}$$

The helicity amplitudes have been split into their vector ($H^V_{\lambda_2\lambda_V}$) and axial-vector ($H^A_{\lambda_2\lambda_V}$) parts. We shall work in the rest frame of the parent baryon B_1 with the daughter baryon B_2 moving in the negative z direction such that $p_1^\mu = (M_1, \mathbf{0})$, $p_2^\mu = (E_2, 0, 0, -|\mathbf{p}_2|)$ and $q^\mu = (q_0, 0, 0, |\mathbf{p}_2|)$. Further $q_0 = (M_+M_- + q^2)/(2M_1)$, $|\mathbf{p}_2| = \sqrt{Q_+Q_-}/2M_1$ and $E_2 = M_1 - q_0 = (M_1^2 + M_2^2 - q^2)/(2M_1)$, where $q^2 = M_V^2$ for the on-mass shell $J/\psi(\psi(2S))$ meson. We have introduced the notation $M_\pm = M_1 \pm M_2$, $Q_\pm = M_\pm^2 - q^2$. Angular momentum conservation fixes the helicity λ_1 of the parent baryon such that $\lambda_1 = -\lambda_2 + \lambda_V$. The relations between the helicity amplitudes $H^{V,A}_{\lambda_2\lambda_V}$ and the invariant amplitudes are given by [32]

$$
\begin{aligned}
H^V_{\pm\frac{1}{2}\pm 1} &= \sqrt{2Q_-}\left(f_1^V + \frac{M_+}{M_1} f_2^V\right),\\
H^A_{\pm\frac{1}{2}\pm 1} &= \pm\sqrt{2Q_+}\left(f_1^A - \frac{M_-}{M_1} f_2^A\right),\\
H^V_{\pm\frac{1}{2}0} &= \sqrt{\frac{Q_-}{q^2}}\left(M_+ f_1^V + \frac{q^2}{M_1} f_2^V\right),\\
H^A_{\pm\frac{1}{2}0} &= \pm\sqrt{\frac{Q_+}{q^2}}\left(M_- f_1^A - \frac{q^2}{M_1} f_2^A\right).
\end{aligned}
\tag{9}
$$

As in Ref. [32] we introduce the following combinations of helicity amplitudes:

$$
\begin{aligned}
H_U &= |H_{\frac{1}{2}1}|^2 + |H_{-\frac{1}{2}-1}|^2 \quad \text{transverse unpolarized},\\
H_L &= |H_{\frac{1}{2}0}|^2 + |H_{-\frac{1}{2}0}|^2 \quad \text{longitudinal unpolarized}.
\end{aligned}
\tag{10}
$$

The partial helicity width corresponding to the two specific combinations of helicity amplitudes in (10) is defined by ($\varepsilon = m_l^2/M_V^2$; $v^2 = 1 - 4\varepsilon$)

$$
\begin{aligned}
&\Gamma_I(\Lambda_b \to \Lambda + V)\\
&\quad = \frac{G_F^2}{32\pi}\frac{|\mathbf{p}_2|}{M_1^2}|V_{cb}V_{cs}^*|^2 C_{\rm eff}^2 f_V^2 M_V^2 v(1+2\varepsilon)H_I\\
&I = U, L.
\end{aligned}
\tag{11}
$$

For the $\Lambda_b \to \Lambda + V$ decay width one finds

$$
\Gamma(\Lambda_b \to \Lambda + V) = \Gamma_U + \Gamma_L. \tag{12}
$$

III. JOINT ANGULAR DECAY DISTRIBUTIONS IN THE CASCADE DECAY $\Lambda_b \to \Lambda(\to p\pi^-) + V(\to \ell^+\ell^-)$

As in the case of the rare meson decays $B \to K^{(*)} + \ell^+\ell^-$ ($\ell = e,\ \mu,\ \tau$) treated in [21] one can exploit the cascade nature of the decay $\Lambda_b(\uparrow) \to \Lambda(\to p\pi^-) + V(\to \ell^+\ell^-)$ of polarized $\Lambda_b(\uparrow)$ decays to write down a fivefold angular decay distribution involving the polar angles θ_1, θ_2 and θ, and the two azimuthal angles ϕ_1 and ϕ_2. V stands for J/ψ or $\psi(2S)$. Since the decay $\psi(2S) \to \tau^+\tau^-$ is kinematically allowed, we include lepton mass effects in our decay formulas. The angular decay distribution involves the helicity amplitudes $h^V_{\lambda_{\ell^+}\lambda_{\ell^-}}$ for the decay $V \to \ell^+\ell^-$, $H_{\lambda_\Lambda\lambda_V}$ for the decay $\Lambda_b \to \Lambda + V$ and $h^B_{\lambda_p 0}$ for the decay $\Lambda \to p + \pi^-$.

We do not write out the full fivefold angular decay distribution that can be found in [35], or that can be adapted from the corresponding fivefold decay distributions for the semileptonic baryon decays $\Xi^0 \to \Sigma^+ + \ell^-\bar\nu_\ell$ and $\Lambda_c \to \Lambda + \ell^+\nu_\ell$ written down in [34,36], respectively. Instead we discuss a threefold polar angle distribution for polarized Λ_b decay and a threefold joint decay distribution for unpolarized Λ_b decay. These can be obtained from the full fivefold decay distributions written down in [34–36] by the appropriate angular integrations or by setting the polarization of the Λ_b to zero.

A. Polar angle distribution in polarized Λ_b decay

Let us first consider the polar angle distribution $W(\theta, \theta_1, \theta_2)$ for polarized Λ_b decays, which has been discussed before in [1,37] in the zero lepton mass approximation (see Fig. 1).

The angular decay distribution can be derived from the master formula

$$
\begin{aligned}
W(\theta,\theta_1,\theta_2) \propto \frac{1}{2}\sum_{\rm helicities} &|h^V_{\lambda_{\ell^+}\lambda_{\ell^-}}|^2 [d^1_{\lambda_V,\lambda_{\ell^+}-\lambda_{\ell^-}}(\theta_2)]^2\\
&\times \rho_{\lambda_{\Lambda_b},\lambda_{\Lambda_b}}(\theta)\delta_{\lambda_{\Lambda_b},\lambda_V-\lambda_\Lambda}|H_{\lambda_\Lambda\lambda_V}|^2\\
&\times [d^{1/2}_{\lambda_\Lambda\lambda_p}(\theta_1)]^2 |h^B_{\lambda_p 0}|^2,
\end{aligned}
\tag{13}
$$

where the summation extends over all possible helicities λ_{ℓ^+}, λ_{ℓ^-}, λ_{Λ_b}, λ_Λ, $\lambda_p = \pm\frac{1}{2}$ and $\lambda_V = 0, \pm 1$. For the diagonal terms of the density matrix $\rho_{\lambda_{\Lambda_b},\lambda_{\Lambda_b}}(\theta)$ appearing in Eq. (13) one has

$$
\rho(\theta) = \frac{1}{2}\,\mathrm{diag}(1 - P_b\cos\theta,\ 1 + P_b\cos\theta). \tag{14}
$$

The vector current lepton helicity amplitudes are given by (see [32])

$$
\begin{aligned}
\text{flip: } h^V_{-\frac{1}{2}-\frac{1}{2}} &= h^V_{+\frac{1}{2}+\frac{1}{2}} = 2m_l,\\
\text{nonflip: } h^V_{-\frac{1}{2}+\frac{1}{2}} &= h^V_{+\frac{1}{2}-\frac{1}{2}} = \sqrt{2q^2}.
\end{aligned}
\tag{15}
$$

Finally, factorizing out the combination $|h^B_{+\frac{1}{2}0}|^2 + |h^B_{-\frac{1}{2}0}|^2 \propto \mathrm{Br}(\Lambda \to p\pi)$ and introducing the asymmetry parameter

$$
\alpha_\Lambda = \frac{|h^B_{+\frac{1}{2}0}|^2 - |h^B_{-\frac{1}{2}0}|^2}{|h^B_{+\frac{1}{2}0}|^2 + |h^B_{-\frac{1}{2}0}|^2}, \tag{16}
$$

one obtains the angular decay distribution

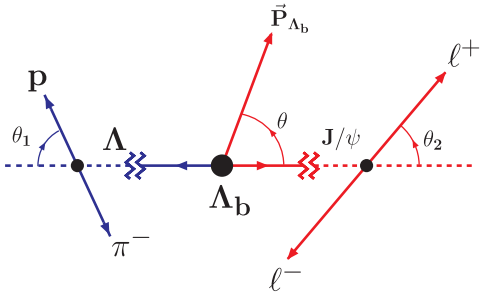

FIG. 1 (color online). Definition of the three polar angles in the cascade decay $\Lambda_b(\uparrow) \to \Lambda(\to p\pi^-) + J/\psi(\to \ell^+\ell^-)$ of a polarized Λ_b baryon.

$$W(\theta,\theta_1,\theta_2) \propto \frac{1}{2}|H_{+\frac{1}{2}1}|^2[q^2(1+\cos^2\theta_2)+4m_l^2\sin^2\theta_2](1-P\cos\theta)(1+\alpha_\Lambda\cos\theta_1)+\frac{1}{2}|H_{-\frac{1}{2}-1}|^2[q^2(1+\cos^2\theta_2)$$
$$+4m_l^2\sin^2\theta_2](1+P\cos\theta)(1-\alpha_\Lambda\cos\theta_1)+|H_{+\frac{1}{2}0}|^2[q^2\sin^2\theta_2+4m_l^2\cos^2\theta_2](1+P\cos\theta)(1+\alpha_\Lambda\cos\theta_1)$$
$$+|H_{-\frac{1}{2}0}|^2(q^2\sin^2\theta_2+4m_l^2\cos^2\theta_2)(1-P\cos\theta)(1-\alpha_\Lambda\cos\theta_1). \quad (17)$$

Following Ref. [1] we introduce linear combinations of normalized squared helicity amplitudes $|\hat{H}_{\lambda_{\Lambda_b}\lambda_V}|^2$ by writing

$$\alpha_b = |\hat{H}_{+\frac{1}{2}0}|^2 - |\hat{H}_{-\frac{1}{2}0}|^2 + |\hat{H}_{-\frac{1}{2}-1}|^2 - |\hat{H}_{+\frac{1}{2}+1}|^2, \qquad r_0 = |\hat{H}_{+\frac{1}{2}0}|^2 + |\hat{H}_{-\frac{1}{2}0}|^2, \qquad r_1 = |\hat{H}_{+\frac{1}{2}0}|^2 - |\hat{H}_{-\frac{1}{2}0}|^2, \quad (18)$$

where $|\hat{H}_{\lambda_{\Lambda_b}\lambda_V}|^2 = |H_{\lambda_{\Lambda_b}\lambda_V}|^2/N$ and where the normalization factor N is given by $N \equiv |H_{+\frac{1}{2}0}|^2 + |H_{-\frac{1}{2}0}|^2 + |H_{-\frac{1}{2}-1}|^2 + |H_{+\frac{1}{2}+1}|^2$. Similar to [1] the angular decay distribution can be rearranged into the form

$$\tilde{W}(\theta,\theta_1,\theta_2) = \sum_{i=0}^{7} f_i(\alpha_b, r_0, r_1) g_i(P_b,\alpha_\Lambda)\, h_i(\cos\theta,\cos\theta_1,\cos\theta_2)\,\ell_i(\varepsilon)$$
$$= v(1+2\varepsilon) + \sum_{i=1}^{7} f_i(\alpha_b, r_0, r_1)\, g_i(P_b,\alpha_\Lambda)\, h_i(\cos\theta,\cos\theta_1,\cos\theta_2)\,\ell_i(\varepsilon), \quad (19)$$

such that the angular factors $h_i(\cos\theta,\cos\theta_1,\cos\theta_2)$ $(i=1,\ldots,7)$ in the second row of Eq. (19) integrate to zero after polar integration. The functions f_i, g_i, h_i and ℓ_i $(i=0,\ldots,7)$ that describe the normalized angular distribution (19) are listed in Table I. Setting $\varepsilon = m_\ell^2/M_V^2$ to zero and the velocity parameter $v = \sqrt{1-4\varepsilon}$ to 1 as is appropriate in the zero lepton mass approximation one recovers Table 2 of Ref. [1]. It is clear that one can determine the four parameters (P_b, α_b, r_0 and r_1) from a global fit to the polar angle distribution as has been done in [1].

TABLE I. Decay functions appearing in the threefold polar angle distribution in the decay of a polarized Λ_b. The velocity is defined as $v = \sqrt{1-4\varepsilon}$. In our numerical analysis we use $\alpha_\Lambda = 0.642$ [11].

i	$f_i(\alpha_b, r_0, r_1)$	$g_i(P_b,\alpha_\Lambda)$	$h_i(\cos\theta,\cos\theta_1,\cos\theta_2)$	$\ell_i(\varepsilon)$
0	1	1	1	$v\cdot(1+2\varepsilon)$
1	α_b	P_b	$\cos\theta$	$v\cdot(1+2\varepsilon)$
2	$2r_1-\alpha_b$	α_Λ	$\cos\theta_1$	$v\cdot(1+2\varepsilon)$
3	$2r_0-1$	$P_b\alpha_\Lambda$	$\cos\theta\cos\theta_1$	$v\cdot(1+2\varepsilon)$
4	$\frac{1}{2}(1-3r_0)$	1	$\frac{1}{2}(3\cos^2\theta_2-1)$	$v\cdot v^2$
5	$\frac{1}{2}(\alpha_b-3r_1)$	P_b	$\frac{1}{2}(3\cos^2\theta_2-1)\cos\theta$	$v\cdot v^2$
6	$-\frac{1}{2}(\alpha_b+r_1)$	α_Λ	$\frac{1}{2}(3\cos^2\theta_2-1)\cos\theta_1$	$v\cdot v^2$
7	$-\frac{1}{2}(1+r_0)$	$P_b\alpha_\Lambda$	$\frac{1}{2}(3\cos^2\theta_2-1)\cos\theta\cos\theta_1$	$v\cdot v^2$

Let us briefly dwell on the powers of the velocity factor v in Table I. The common factor v in the fifth column of Table I has its origin in the phase space factor v in the decay $V\to\ell^+\ell^-$. The remaining v dependence results from a dominant S-wave contribution in the factor $(1+2\varepsilon)$ and a dominant $S-D$-interference contribution in the factor $v^2=(1-4\varepsilon)$, respectively, as can be seen by performing an LS analysis of the decay $V\to\ell^+\ell^-$. The LS amplitudes M_{LS} are given by $M_{01} = \sqrt{2/3}(h^V_{+\frac{1}{2}+\frac{1}{2}} + \sqrt{2}h^V_{+\frac{1}{2}-\frac{1}{2}})$ and $M_{21} = \sqrt{2/3}(-\sqrt{2}h^V_{+\frac{1}{2}+\frac{1}{2}} + h^V_{+\frac{1}{2}-\frac{1}{2}})$. One then finds

$$1+2\varepsilon = \frac{1}{4q^2}(M_{01}^2+M_{21}^2),$$
$$v^2 = 1-4\varepsilon = \frac{1}{4q^2}M_{21}(2\sqrt{2}M_{01}-M_{21}). \quad (20)$$

By integrating over two respective angles of the three polar angles one obtains the single angle distributions $W(\theta)$, $W(\theta_1)$ and $W(\theta_2)$. In their normalized forms they read

$$\hat{W}(\theta) = \frac{1}{2}(1+\alpha_b P_b\cos\theta), \quad (21)$$

$$\hat{W}(\theta_1) = \frac{1}{2}(1+2(2r_1-\alpha_b)\alpha_\Lambda\cos\theta_1), \quad (22)$$

TABLE II. Numerical values of the velocity v and the velocity factors $\ell_i(\varepsilon)$.

	$J/\psi\to\mu^+\mu^-$	$\psi(2S)\to\mu^+\mu^-$	$\psi(2S)\to\tau^+\tau^-$
v	0.998	0.998	0.266
$v(1+2\varepsilon)$ $(i=0,\ldots,3)$	1.000	1.000	0.389
v^3 $(i=4,\ldots,7)$	0.993	0.995	0.019

$$\hat{W}(\theta_2) = \frac{1}{2(1+2\varepsilon)} \times \left((1+2\varepsilon) + \frac{1}{4}(1-4\varepsilon)(1-3r_0)(3\cos^2\theta_2 - 1)\right), \tag{23}$$

where the factor

$$(2r_1 - \alpha_b) = |\hat{H}_{+\frac{1}{2}0}|^2 + |\hat{H}_{+\frac{1}{2}1}|^2 - |\hat{H}_{-\frac{1}{2}0}|^2 - |\hat{H}_{-\frac{1}{2}-1}|^2 = P_\Lambda^\ell \tag{24}$$

defines the longitudinal polarization of the daughter baryon Λ and the factor

$$(1-3r_0) = -2(|\hat{H}_{+\frac{1}{2}0}|^2 + |\hat{H}_{-\frac{1}{2}0}|^2) + |\hat{H}_{+\frac{1}{2}1}|^2 + |\hat{H}_{-\frac{1}{2}-1}|^2 \tag{25}$$

is a measure of the longitudinal/transverse polarization composition of the vector charmonium state. Since the decay $V \to \ell^+\ell^-$ is electromagnetic and therefore parity conserving, the decay is not sensitive to the difference of the transverse-plus and transverse-minus helicity contributions $|\hat{H}_{+\frac{1}{2}+1}|^2 - |\hat{H}_{-\frac{1}{2}-1}|^2$. For the same reason there is no linear $\cos\theta_2$ contribution in Eq. (23).

The distributions $\hat{W}(\theta)$ and $\hat{W}(\theta_1)$ are asymmetric in $\cos\theta$ and $\cos\theta_1$ such that they can be characterized by the forward-backward (FB) asymmetries

$$A_{\rm FB}|_\theta = \frac{1}{2}\alpha_b P_b, \tag{26}$$

$$A_{\rm FB}|_{\theta_1} = (2r_1 - \alpha_b)\alpha_\Lambda. \tag{27}$$

The distribution $\hat{W}(\theta_2)$ is symmetric in $\cos\theta_2$ with its convexity parameter c_f given by

$$c_f = \frac{d^2\hat{W}(\cos\theta_2)}{d(\cos\theta_2)^2} = \frac{3}{4}\frac{(1-4\varepsilon)}{(1+2\varepsilon)}(1-3r_0). \tag{28}$$

In Table II we have listed the numerical values of the two velocity factors $v(1+2\varepsilon)$ and v^3 for the cases involving the muon and the tau lepton. It is quite apparent that the zero lepton mass approximation is quite good for $J/\psi \to \mu^+\mu^-$ and $\psi(2S) \to \mu^+\mu^-$. For the case $\psi(2S) \to \tau^+\tau^-$ the factor $v(1+2\varepsilon)$ provides a reduction of about 60% relative to the e^+e^- and $\mu^+\mu^-$ cases while the factor v^3 becomes negligibly small. This means that for $\psi(2S) \to \tau^+\tau^-$ one loses the analyzing power of the lepton-side decay, i.e. of the last four rows of Table I. For the same reason, one will have an almost flat decay distribution $\hat{W}(\cos\theta_2)$ for $\psi(2S) \to \tau^+\tau^-$ because of the factor $v^2 = 1 - 4\varepsilon$ in the expression Eq. (28) for the convexity parameter.

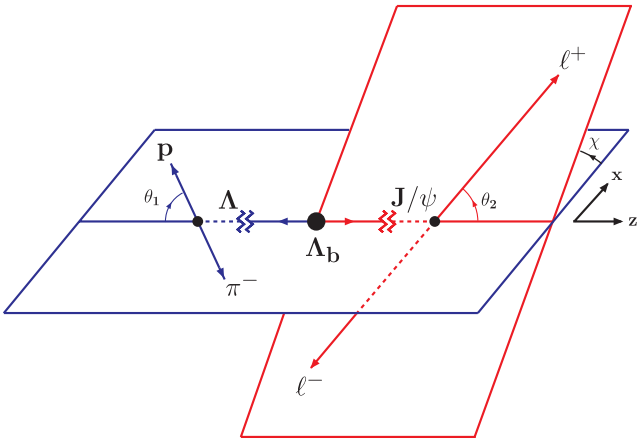

FIG. 2 (color online). Definition of two polar angles θ_1, θ_2 and one azimuthal angle χ in the cascade decay $\Lambda_b \to \Lambda(\to p\pi^-) + J/\psi(\to \ell^+\ell^-)$ of an unpolarized Λ_b.

B. Azimuthal angle distribution

Consider the angular decay distribution of an unpolarized Λ_b that is characterized by the two polar angles (θ_1) and (θ_2), and an azimuthal angle χ defined by the azimuth of the two decay planes defined by the decays $V \to \ell^+\ell^-$ and $\Lambda \to p\pi^-$ (see Fig. 2). The angular decay distribution can then be calculated from the master formula

$$W(\theta_1,\theta_2,\chi) \propto \sum_{\rm helicities} |h^V_{\lambda_1\lambda_2}|^2 e^{i(\lambda_V - \lambda'_V)\chi} d^1_{\lambda_V,\lambda_1-\lambda_2}(\theta_2) d^1_{\lambda'_V,\lambda_1-\lambda_2}(\theta_2) \delta_{\lambda_V-\lambda_\Lambda,\lambda'_V-\lambda'_\Lambda} H_{\lambda_\Lambda\lambda_V} H^\dagger_{\lambda'_\Lambda\lambda'_V} d^{1/2}_{\lambda_\Lambda\lambda_p}(\theta_1) d^{1/2}_{\lambda'_\Lambda\lambda_p}(\theta_1) |h^B_{\lambda_p 0}|^2. \tag{29}$$

Let us first present a qualitative argument that the azimuthal correlation between the two decay planes is small. Azimuthal correlations result from the configurations $\lambda_V - \lambda'_V = \pm 1$. This implies that $\lambda_\Lambda = -\lambda'_\Lambda$ following from the δ-function condition $\lambda_V - \lambda_\Lambda = \lambda'_V - \lambda'_\Lambda$, which again follows from the fact that Λ_b is treated as unpolarized. The azimuthal correlations are therefore determined by bilinear forms such as $H_{\frac{1}{2}\lambda_V} H^\dagger_{-\frac{1}{2}\lambda'_V}$ with $\lambda_V \neq \lambda'_V$. We shall see in Sec. VI that in general $|H_{\frac{1}{2}\lambda_V}| \ll |H_{-\frac{1}{2}\lambda'_V}|$ (as also expected from the naive quark model) such that one concludes that the azimuthal correlations between the two decay planes are quite small.

Let us cast this reasoning into a more quantitative form. The threefold angular decay distribution resulting from Eq. (29) reads

$$
\begin{aligned}
W(\theta_1,\theta_2,\chi) = {} & \frac{3}{8}(1+\cos^2\theta_2)(|H_{\frac{1}{2}1}|^2(1+\alpha_\Lambda\cos\theta_1)+|H_{-\frac{1}{2}-1}|^2(1-\alpha_\Lambda\cos\theta_1)) \\
& + \frac{3}{4}\sin^2\theta_2(|H_{\frac{1}{2}0}|^2(1+\alpha_\Lambda\cos\theta_1)+|H_{-\frac{1}{2}0}|^2(1-\alpha_\Lambda\cos\theta_1)) \\
& + \frac{4m_\ell^2}{q^2}\Big[\frac{3}{8}\sin^2\theta_2(|H_{\frac{1}{2}1}|^2(1+\alpha_\Lambda\cos\theta_1)+|H_{-\frac{1}{2}-1}|^2(1-\alpha_\Lambda\cos\theta_1)) \\
& + \frac{3}{4}\cos^2\theta_2(|H_{\frac{1}{2}0}|^2(1+\alpha_\Lambda\cos\theta_1)+|H_{-\frac{1}{2}0}|^2(1-\alpha_\Lambda\cos\theta_1))\Big] \\
& + \left(1-\frac{4m_\ell^2}{q^2}\right)\frac{3}{4\sqrt{2}}\alpha_\Lambda\sin 2\theta_2\sin\theta_1(\cos\chi\,\mathrm{Re}[H_{\frac{1}{2}1}H^\dagger_{-\frac{1}{2}0}-H_{-\frac{1}{2}-1}H^\dagger_{\frac{1}{2}0}] \\
& - \sin\chi\,\mathrm{Im}[H_{\frac{1}{2}1}H^\dagger_{-\frac{1}{2}0}+H_{-\frac{1}{2}-1}H^\dagger_{\frac{1}{2}0}]). \qquad (30)
\end{aligned}
$$

Integrating over the hadron-side polar angle θ_1 one obtains

$$
\begin{aligned}
W(\theta_2,\chi) = {} & \frac{3}{8}(1+\cos^2\theta_2)\cdot 2(|H_{\frac{1}{2}1}|^2+|H_{-\frac{1}{2}-1}|^2)+\frac{3}{4}\sin^2\theta_2\cdot 2(|H_{\frac{1}{2}0}|^2+|H_{-\frac{1}{2}0}|^2) \\
& + \frac{4m_\ell^2}{q^2}\Big[\frac{3}{8}\sin^2\theta_2\cdot 2(|H_{\frac{1}{2}1}|^2+|H_{-\frac{1}{2}-1}|^2)+\frac{3}{4}\cos^2\theta_2\cdot 2(|H_{\frac{1}{2}0}|^2+|H_{-\frac{1}{2}0}|^2)\Big] \\
& + \left(1-\frac{4m_\ell^2}{q^2}\right)\frac{3}{4\sqrt{2}}\frac{\pi}{2}\alpha_\Lambda\sin 2\theta_2(\cos\chi\,\mathrm{Re}(H_{\frac{1}{2}1}H^\dagger_{-\frac{1}{2}0}-H_{-\frac{1}{2}-1}H^\dagger_{\frac{1}{2}0})-\sin\chi\,\mathrm{Im}(H_{\frac{1}{2}1}H^\dagger_{-\frac{1}{2}0}+H_{-\frac{1}{2}-1}H^\dagger_{\frac{1}{2}0})). \qquad (31)
\end{aligned}
$$

If one wants to define a measure of the azimuthal correlation, one cannot integrate Eq. (31) over the whole range of the lepton-side polar angle θ_2 because $\int_{-1}^{1} d\cos\theta_2 \sin 2\theta_2 = 0$. However, one can recover a nonzero azimuthal correlation measure by defining a FB asymmetry with respect to the lepton-side polar angle θ_2 by writing

$$
A_{\rm FB}(\chi) = \frac{F-B}{F+B}. \qquad (32)
$$

On reintroducing the normalized helicity amplitudes one obtains

$$
\begin{aligned}
A_{\rm FB}(\chi) = {} & \frac{(1-4\varepsilon)}{(1+2\varepsilon)}\frac{\pi}{8\sqrt{2}}\alpha_\Lambda(\cos\chi\,\mathrm{Re}[\hat{H}_{\frac{1}{2}1}\hat{H}^\dagger_{-\frac{1}{2}0}-\hat{H}_{-\frac{1}{2}-1}\hat{H}^\dagger_{\frac{1}{2}0}] \\
& - \sin\chi\,\mathrm{Im}[\hat{H}_{\frac{1}{2}1}\hat{H}^\dagger_{-\frac{1}{2}0}+\hat{H}_{-\frac{1}{2}-1}\hat{H}^\dagger_{\frac{1}{2}0}]). \qquad (33)
\end{aligned}
$$

IV. THE $\Lambda_b \to \Lambda$ FORM FACTORS IN THE COVARIANT CONFINED QUARK MODEL

For the description of the couplings of the baryons Λ_Q ($Q = b,\ s$) and the charmonium vector meson states $V = J/\psi,\ \psi(2S)$ to their three and two constituent quarks, respectively, we employ a generic Lagrangian that reads

$$
\begin{aligned}
& \Lambda_Q\colon\ \mathcal{L}^{\Lambda_Q}_{\rm int}(x) = g_{\Lambda_Q}\bar{\Lambda}_Q(x)\cdot J_{\Lambda_Q}(x) + \mathrm{H.c.}, \\
& J_{\Lambda_Q}(x) = \int dx_1\int dx_2\int dx_3 F_{\Lambda_Q}(x;x_1,x_2,x_3) \\
& \times \epsilon^{a_1a_2a_3}Q^{a_1}(x_1)u^{a_2}(x_2)C\gamma^5 d^{a_3}(x_3), \qquad (34) \\
& V\colon\ \mathcal{L}^{V}_{\rm int}(x) = g_V V(x)\cdot J_V(x), \\
& J_V(x) = \int dx_1\int dx_2 F_V(x;x_1,x_2)\bar{c}^a(x_1)\gamma^\mu c^a(x_2). \qquad (35)
\end{aligned}
$$

The color index is denoted by a, and $C = \gamma^0\gamma^2$ is the charge conjugation matrix. In the baryon case we take the u and d quarks to be in a $[ud]$ diquark configuration antisymmetric in spin and isospin. We emphasize, however, that we treat the u and d quarks as separate dynamical entities and not as a dynamical diquark state. Vertex functions in momentum space are obtained from the Fourier transformations of the vertex functions F_H in Eqs. (34) and (35). In the numerical calculations we choose a simple Gaussian form for the vertex functions (for both mesons and baryons),

$$
\bar{\Phi}_H(-P^2) = \exp(P^2/\Lambda_H^2), \qquad (36)
$$

where Λ_H is a size parameter describing the distribution of the quarks inside a given hadron H. We use the values of these parameters fixed before in [29,30,32]. We would like to stress that the Minkowskian momentum variable P^2 turns into the Euclidean form $-P_E^2$ needed for the

appropriate falloff behavior of the correlation function (36) in the Euclidean region. We emphasize that any choice for the correlation function $\bar{\Phi}_H$ is acceptable as long as it falls off sufficiently fast in the ultraviolet region of Euclidean space. The choice of a Gaussian form for $\bar{\Phi}_H$ has obvious calculational advantages.

For given values of the size parameters Λ_H the coupling constants g_{Λ_Q} and g_V are determined by the compositeness condition suggested by Weinberg [38] and Salam [39] (for a review, see [40]) and extensively used in our approach (for details, see [41]). The compositeness condition implies that the renormalization constant of the hadron wave function is set equal to zero,

$$Z_H = 1 - \Sigma_H' = 0, \tag{37}$$

where Σ_H' is the on-shell derivative of the hadron mass function Σ_H with respect to its momentum. The compositeness condition can be seen to provide for the correct charge normalization for a charged bound state (see e.g. [29]).

Next we discuss the calculation of the matrix element of the $\Lambda_b \to \Lambda + V$ transition. We work in the so-called factorization approximation in which the matrix element for $\Lambda_b \to \Lambda + V$ factorizes into a $(b \to s)$ current-induced matrix element $\langle \Lambda | J^\mu | \Lambda_b \rangle$ and a $(c \to c)$ current-induced vacuum to vector meson matrix element $\langle V | J^\mu | 0 \rangle$. In our approach the $\Lambda_b \to \Lambda$ transition is described by a two-loop Feynman-type diagram, and the current-induced vacuum to vector meson transition is described by a one-loop Feynman-type diagram. The latter diagram is proportional to the leptonic decay constant of the vector meson denoted by f_V. We have calculated $f_{J/\psi}$ before in Ref. [29] and have found $f_J = 415$ MeV in almost perfect agreement with the measured value. In the calculation of quark-loop diagrams we use the set of model parameters fixed in our previous studies. The model parameters are the constituent quark masses m_q and the infrared cutoff parameter λ responsible for quark confinement. They are taken from a fit done in the papers [29,30],

$$\begin{array}{ccccccc} m_u & & m_s & m_c & m_b & \lambda & \\ 0.235 & & 0.424 & 2.16 & 5.09 & 0.181 & \text{GeV} \end{array}. \tag{38}$$

The dimensional size parameters of the Λ_b and Λ baryons have been determined in [32] by a fit to the semileptonic decays $\Lambda_b \to \Lambda_c + \ell^- \bar{\nu}_\ell$ and $\Lambda_c \to \Lambda + \ell^+ \nu_\ell$. The resulting values are $\Lambda_\Lambda = 0.490$ GeV, and $\Lambda_{\Lambda_b} = 0.569$ GeV. For the size parameter of the J/ψ we take $\Lambda_{J/\psi} = 1.482$ GeV resulting from the fit in [29]. As of yet we cannot treat radial excitations in our approach. We therefore take the experimental value $f_{\psi(2S)} = 286.7$ MeV for the $\psi(2S)$.

It should be quite clear that the evaluation of the form factors is technically quite involved since it involves the calculation of a two-loop Feynman diagram with a complex spin structure resulting from the quark propagators and the vertex functions, which leads to a number of two-loop tensor integrals. To tackle this difficult task we have automated the calculation in the form of FORM [42] and FORTRAN packages written for this purpose. The q^2 behavior of the form factors are shown in Fig. 3.

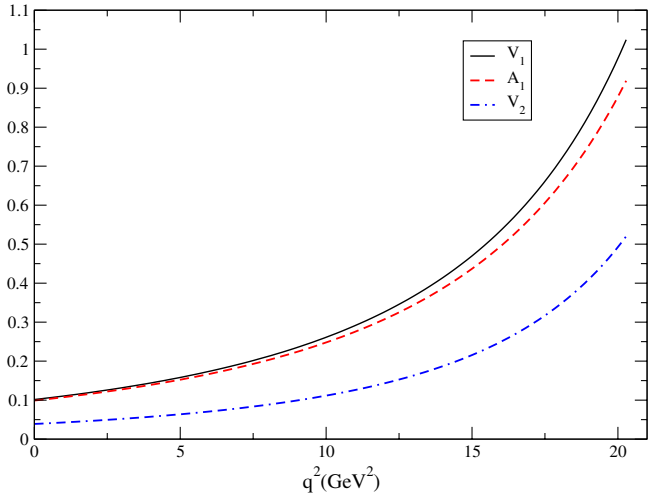

FIG. 3 (color online). q^2 dependence of the three form factors $V_1 \equiv f_1^V(q^2)$, $A_1 \equiv f_1^A(q^2)$ and $V_2 \equiv f_2^V(q^2)$. The form factor $A_2 \equiv f_2^A(q^2)$ is not shown since it would not be visible at the scale of the figure. The values of $q^2 = 0$ and $q^2 = q^2_{\rm max}$ correspond to the maximal and minimal recoil points, respectively.

The results of our numerical calculations are well represented by a double-pole parametrization

$$f(\hat{s}) = \frac{f(0)}{1 - a\hat{s} + b\hat{s}^2}, \tag{39}$$

where $\hat{s} = q^2/M^2_{\Lambda_b}$. Using such a parametrization facilitates further treatment such as the q^2 integrations without having to do a numerical evaluation for each q^2 value separately. The values of $f(0)$, a and b are listed in Table III. It is quite noteworthy that the numerical values of a and b for each form factor in Table III are approximately related by $\sqrt{b} \approx a/2$ such that the ensuing form factors are of approximate dipole form. The relevant scale of the effective dipole form factors is determined by $m_{\rm dipole} = m_{\Lambda_b}/\sqrt{r}$ where r is taken to be the average of $\sqrt{b}$ and $a/2$; i.e. we take $r = (\sqrt{b} + a/2)/2$. The corresponding mass scale $m_{\rm dipole}$ of the effective dipole form factor is then given by $m_{\rm dipole} = m_{\Lambda_b}/r$. One calculates

TABLE III. Parameters for the approximated form factors in Eq. (39) in $\Lambda_b \to \Lambda$ transitions.

	f_1^V	f_2^V	f_1^A	f_2^A
$f(0)$	0.107	0.043	0.104	−0.003
a	2.271	2.411	2.232	2.955
b	1.367	1.531	1.328	3.620

TABLE IV. Comparison of our form factor values at $q^2 = 0$, $q^2 = m^2_{J/\psi}$ and $q^2 = q^2_{\rm max}$ with those obtained in [9,10].

		f_1^V	f_2^V	f_3^V	f_1^A	f_2^A	f_3^A
$q^2 = 0$	[9]	0.1081	0.0311		0.1065	0.0064	
	[10]	0.025	0.017	−0.0053	0.028	0.0049	−0.019
	our	0.10	0.039	−0.0017	0.099	0.0036	−0.047
$q^2 = m^2_{J/\psi}$	[9]	0.248	0.105		0.249	0.0214	
	[10]	0.255	0.100	−0.044	0.237	0.020	−0.136
	our	0.25	0.11	−0.0097	0.24	−0.0066	−0.13
$q^2 = q^2_{\rm max}$	[9]	0.532	0.204		0.613	0.0471	
	[10]	0.903	0.256	0.054	0.869	−0.072	−0.308
	our	1.02	0.52	−0.099	0.92	−0.0018	−0.67

$m_{\rm dipole} = 5.23$, 5.08, 5.28 and 4.32 GeV for the four form factors in Table III. It is quite gratifying that for each case the effective dipole masses come out to be close to the average weighted mass $(m_{B_s} + 3m_{B_s^*}/4) = 5.31$ GeV of the ground state $(b\bar{s})$ mesons, which would set the scale for the q^2 behavior of the form factors in a generalized vector dominance picture.

In Table IV we list our form factor results for three different values of q^2 and compare them to the results of the light-front diquark model calculation of [9] and the potential quark model calculation of [10]. At $q^2 = m^2_{J/\psi}$ all three model form factors agree for the large form factors f_1^V and f_1^A, while the small form factors f_2^V and f_2^A of [9] differ from those of the other two models. There are larger discrepancies of the three sets of form factors for the other two q^2 values. In particular, at $q^2_{\rm max}$ the form factor values of [9] are much smaller than those of the other two models, while at $q^2 = 0$ the large form factors f_1^V and f_1^A of [10] come out much smaller than in the two other models. The $q^2 = 0$ values of our form factors in Table III slightly differ from those in Table IV because the former are fit results while the latter are full model results. The values of the form factors at $q^2 = m^2_{J/\psi}$ show that the effective interaction of the $\Lambda_b \to \Lambda$ transition is very close to a $(V - A)$ form in all three models.

At maximum recoil $q^2 = 0$ we can compare our results with the light-cone sum rules (LCSR) results of [43] on the $\Lambda_b \to p$ transition form factors if we assume $SU(3)$ to hold. In the limit of $SU(3)$ the $\Lambda_b \to \Lambda$ and $\Lambda_b \to p$ form factors are related by $F(\Lambda_b \to \Lambda) = \sqrt{2/3} F(\Lambda_b \to p)$. This can be seen by using the $\bar{3} \otimes 3 \to 8$ Clebsch-Gordan (C.G.) table listed in [44]. Based on the observation that the $[ud]$ diquark is the $(Y = 2/3, I = 0)$ member of the $\bar{3}$ multiplet one needs the C.G. coefficients

$$\Lambda_b \to \Lambda: \left\langle \bar{\mathbf{3}}, \frac{2}{3}, 0, 0; \mathbf{3}, -\frac{2}{3}, 0, 0 | \mathbf{8}, 0, 0, 0 \right\rangle = \sqrt{2/3},$$
$$\Lambda_b \to p: \left\langle \bar{\mathbf{3}}, \frac{2}{3}, 0, 0; \mathbf{3}, \frac{1}{3}, \frac{1}{2}, \frac{1}{2} | \mathbf{8}, 1, \frac{1}{2}, \frac{1}{2} \right\rangle = 1. \tag{40}$$

The labeling in (40) proceeds according to the sequence $|\boldsymbol{R}, Y, I, I_z\rangle$ where $\boldsymbol{R}$ denotes the relevant $SU(3)$ representation.

The LCSR results of [43] have been summarized in Table 1 of [45]. We take central values of the results listed in [45] and average over the two options of Λ_b currents. We finally multiply these numbers by $\sqrt{2/3}$ and obtain $f_1^V = 0.11\,(0.10)$, $f_2^V = 0.041\,(0.039)$, $f_1^A = 0.11\,(0.099)$ and $f_2^A = 0.018\,(-0.0036)$ where we have added our model predictions in brackets. The agreement is quite satisfactory except for the small form factor f_2^A where we obtain a smaller value that differs in sign from that in [45].

V. THE HEAVY QUARK LIMIT FOR THE $\Lambda_b \to \Lambda$ FORM FACTORS

It is instructive to explore the HQL for the heavy-to-light transition $\Lambda_b \to \Lambda$ in our form factor expressions. The HQL corresponds to the limit $m_{\Lambda_b}, m_b \to \infty$ while keeping the difference $m_{\Lambda_b} - m_b = \bar{\Lambda}$ and the size parameter Λ_{Λ_b} fixed. The limit has to be taken in the relevant expressions for the coupling constants and the form factors.

First consider the local b-quark propagator that reduces to the static form

$$S_b(k_1 + p_1) = \frac{1}{m_b - \not{k}_1 - \not{p}_1} \to \frac{1 + \not{v}_1}{-2k_1 v_1 - 2\bar{\Lambda}} + \mathcal{O}\left(\frac{1}{m_b}\right), \tag{41}$$

in the HQL. In Eq. (41) p_1 and $v_1 = p_1/m_{\Lambda_b}$ denote the momentum and the four-velocity of the Λ_b. The momentum k_1 is the loop momentum running through the loop involving the $b \to s$ transition. The value of the parameter $\bar{\Lambda} = m_{\Lambda_b} - m_b$ is fixed by our overall fit value for the b-quark mass [see Eq. (38)].

Next consider the b-quark mass dependence of the vertex function $F_{\Lambda_Q}(x; x_1, x_2, x_3)$ in Eq. (34). In our model the vertex function reads

$$F_{\Lambda_Q}(x; x_1, x_2, x_3) = \delta^{(4)}\left(x - \sum_{i=1}^{3} w_i x_i\right) \Phi_{\Lambda_Q}\left(\sum_{i<j} (x_i - x_j)^2\right), \tag{42}$$

where Φ_{Λ_Q} is the correlation function of the three constituent quarks with the coordinates x_1, x_2, x_3 and the masses m_1, m_2, m_3, respectively. The variable w_i is defined by $w_i = m_i/(m_1 + m_2 + m_3)$ such that $\sum_{i=1}^3 w_i = 1$. In the present application $m_1 = m_b$, $m_2 = m_u$ and $m_3 = m_d$. In the limit $m_1 \to \infty$ one has

$$w_1 = 1 - \frac{m_2 + m_3}{m_1} + \mathcal{O}\left(\frac{1}{m_1^2}\right), \qquad w_2 = \frac{m_2}{m_1} + \mathcal{O}\left(\frac{1}{m_1^2}\right),$$
$$w_3 = \frac{m_3}{m_1} + \mathcal{O}\left(\frac{1}{m_1^2}\right). \tag{43}$$

As it turns out, the next-to-leading order corrections $\frac{m_2}{m_1}$ and $\frac{m_3}{m_1}$ contribute significantly to the HQL and cannot be neglected in the numerical calculations. On the other hand, we must keep such terms because the terms $p_1 w_2 \sim m_2$ and $p_1 w_3 \sim m_3$ occurring in the vertex function do not vanish in the heavy quark limit (where p_1 is the momenta of the Λ_b baryon).

In the HQL the coupling constant g_{Λ_Q} does not depend on the b-quark mass and the Λ_b mass [there is a dependence on the $\mathcal{O}(m_Q^0)$ parameters—$\bar{\Lambda}$ and Λ]. This is specific to the three-quark system. For example, in the meson case the meson-quark coupling constant scales as $\sqrt{m_b}$ when $m_b \to \infty$. The constancy of g_{Λ_Q} in the HQL will be used to demonstrate the validity of the HQL for the transition form factors. First, we stress that the Ward identity relating the derivative of the mass operator and the electromagnetic vertex function at $p_1 = p_2$ for the heavy baryon with charge ± 1 is still valid. To show the validity of the Ward identity we consider the charged baryon Λ_c (the heavy quark symmetry partner of the Λ_b baryon), which has the charge $e_{\Lambda_c} = 1$. Using a Ward identity one can rewrite the compositeness condition $Z_{\Lambda_c} = 0$ for the heavy Λ_c baryon, in the form (see Ref. [32])

$$\begin{aligned} \bar{u}_{\Lambda_c}(p)\Lambda^{\mu}_{\Lambda_c}(p,p)u_{\Lambda_c}(p) &= \bar{u}_{\Lambda_c}(p)\gamma^{\mu}u_{\Lambda_c}(p), \\ \not{p}u_{\Lambda_c}(p) &= m_{\Lambda_c}u_{\Lambda_c}(p), \end{aligned} \tag{44}$$

where the electromagnetic vertex function $\Lambda^{\mu}_{\Lambda_c}(p,p)$ obtains contributions from the electromagnetic current coupling to the quark lines (triangle contributions) and the vertices (bubble contributions) (see Ref. [32] for details). To make the HQL more transparent we perform a shift of the loop momenta $k_1 \to k_1 + (w_2 + w_3)p$ and $k_2 \to k_2 + w_2 p$. One has

$$\begin{aligned} \Lambda^{\mu}_{\Lambda_c}(p,p) &= 6g^2_{\Lambda_c}\langle\langle e_1 A_1^{\mu} - e_2 A_2^{\mu} + e_3 A_3^{\mu}\rangle\rangle \\ &\quad + 8g^2_{\Lambda_c} s_{\Lambda_c}\langle\langle [Q_1(k_1^{\mu} + (w_2+w_3)p^{\mu}) \\ &\quad + Q_2(k_2^{\mu} + w_2 p^{\mu})]A_0\rangle\rangle, \end{aligned} \tag{45}$$

where the double bracket notation $\langle\langle \cdots \rangle\rangle$ stands for the two integrations over the loop momenta (see Ref. [32]).

Also we use the definitions

$$\begin{aligned} Q_1 &= e_1(w_2 + 2w_3) - e_2(w_1 - w_3) - e_3(2w_1 + w_2), \\ Q_2 &= e_1(w_2 - w_3) - e_2(w_1 + 2w_3) + e_3(w_1 + 2w_2), \\ e_1 &\equiv e_c = \frac{2}{3}, \qquad e_2 \equiv e_u = \frac{2}{3}, \qquad e_3 \equiv e_d = -\frac{1}{3}, \end{aligned} \tag{46}$$

and

$$\begin{aligned} A_0 &= \bar{\Phi}^2_{\Lambda_Q}(-z_0)S_1(k_1+p)\,\mathrm{tr}[S_2(k_2)\gamma^5 S_3(k_2-k_1)\gamma^5], \\ A_1^{\mu} &= \bar{\Phi}^2_{\Lambda_Q}(-z_0)S_1(k_1+p)\gamma^{\mu}S_1(k_1+p) \\ &\quad \times \mathrm{tr}[S_2(k_2)\gamma^5 S_3(k_2-k_1)\gamma^5], \\ A_2^{\mu} &= \bar{\Phi}^2_{\Lambda_Q}(-z_0)S_1(k_1+p) \\ &\quad \times \mathrm{tr}[S_2(k_2)\gamma^{\mu}S_2(k_2)\gamma^5 S_3(k_2-k_1)\gamma^5], \\ A_3^{\mu} &= \bar{\Phi}^2_{\Lambda_Q}(-z_0)S_1(k_1+p) \\ &\quad \times \mathrm{tr}[S_2(k_2)\gamma^5 S_3(k_2-k_1)\gamma^{\mu}S_3(k_2-k_1)\gamma^5]. \end{aligned} \tag{47}$$

Here $s_{\Lambda_Q} \equiv 1/\Lambda^2_{\Lambda_Q}$ and the argument of the vertex function is

$$z_0 = \frac{1}{2}(k_1 - k_2 + w_3 p)^2 + \frac{1}{6}(k_1 + k_2 + (2w_2 + w_3)p)^2. \tag{48}$$

The calculational techniques of the matrix elements in the heavy quark limit can easily be demonstrated for the example of the structure integral occurring in the heavy meson case (the extension to the heavy baryon case is straightforward)

$$I_2(\bar{\Lambda}) = \int \frac{d^4k}{i\pi^2} e^{sk^2} S_Q(k_1+p)\frac{1}{m^2 - k^2}, \tag{49}$$

where $s = 1/\Lambda^2$. For simplicity we only keep the product of the heavy quark propagator and the denominator of the light quark propagator. We start with the Schwinger representation for the quark propagators assuming that both loop and external momenta are Euclidean. In the Euclidean region the denominator of the quark propagator is positive and the integral over the Schwinger parameter is absolutely convergent. However, to use the Schwinger representation for the heavy quark propagator in Eq. (41) in a straightforward way is not quite correct because the HQL has to be taken in Minkowski space where the denominator is not necessarily positive. We will use the heavy quark propagator in the form

$$S_Q(k_1+p) = m_Q(1+\not{v})\int_0^{\infty} d\alpha e^{-\alpha(m_Q^2 - (k_1+p)^2)}, \tag{50}$$

assuming again that all momenta in the exponential are in the Euclidean region. For the numerator of the heavy quark propagator we take the HQL: $m_Q + \not{k} + \not{p} \to m_Q(1+\not{v})$. Next we demonstrate how to proceed with the HQL for such a representation. As mentioned above, we start in the Euclidean region where $k^2 \le 0$ and $(k+p)^2 \le 0$. By using Schwinger's representation for the heavy quark propagator and the denominator of the light quark propagator, scaling the Schwinger parameters $\alpha_i \to t\alpha_i$ and imposing an infrared cutoff, we arrive at

$$I_2(\bar{\Lambda}) = m_Q(1+\not{v})\int_0^{1/\lambda^2} dt\frac{t}{(s+t)^2} \times \int_0^1 d\alpha e^{-t(\alpha m_Q^2+(1-\alpha)m^2-\alpha(1-\alpha)p^2)+\frac{st}{s+t}\alpha^2 p^2}. \quad (51)$$

We will use this representation for the analytical continuation to the physical region $p^2 = (m_Q + \bar{\Lambda})^2$ with $m_Q \to \infty$. Note that in a theory without a cutoff ($\lambda \to 0$) the integral $I_2(\bar{\Lambda})$ has a branch point at $\bar{\Lambda} = m$. The confinement ansatz allows one to remove this singularity. Then we scale the integration variable $\alpha \to \alpha/m_Q$ with $m_Q \to \infty$. Finally, one has

$$I_2(\bar{\Lambda})|_{m_Q\to\infty} \to I_2^{\rm HQL}(\bar{\Lambda}) = (1+\not{v})\int_0^{1/\lambda^2} dt\frac{t}{(s+t)^2}\int_0^\infty d\alpha e^{-t(\alpha^2-2\alpha\bar{\Lambda}+m^2)+\frac{st}{s+t}\alpha^2}. \quad (52)$$

The calculation of the HQL for the coupling constant g_{Λ_b} and the transition form factors $\Lambda^\mu_{\Lambda_b\to\Lambda}(p_1, p_2)$ proceed in the described way. All analytical calculations are done by FORM [42] and the numerical calculations are done using FORTRAN. One finds

$$g_{\Lambda_b} = \begin{cases} 65.23\ \text{GeV}^{-2} & \text{exact}, \\ 59.44\ \text{GeV}^{-2} & \text{HQL}. \end{cases} \quad (53)$$

The coupling constant in the HQL is smaller than the exact coupling constant only by about 10%, which shows that one is quite close to the HQL for the $\Lambda_b \to \Lambda$ transitions. When calculating the HQL for the coupling constant it is important to keep the numerical value of the parameter $\bar{\Lambda}_b$ fixed at its physical value $\bar{\Lambda}_b = m_{\Lambda_b} - m_b = 0.53$ GeV. In fact, the value of $g^{\rm HQL}_{\Lambda_b}$ depends very sensitively on the choice of the parameter $\bar{\Lambda}_b$. For example, if one puts $\bar{\Lambda}_b = 0$, then one calculates $g^{\rm HQL}_{\Lambda_b} = 185.36\ \text{GeV}^{-2}$, which differs significantly from the exact result $g_{\Lambda_b} = 65.23\ \text{GeV}^{-2}$. This demonstrates how important it is to keep the physical value of $\bar{\Lambda}_b$. It is interesting to compare our results for the coupling constants g_{Λ_b} and g_{Λ_c}. For g_{Λ_c} one finds

$$g_{\Lambda_c} = \begin{cases} 69.88\ \text{GeV}^{-2} & \text{exact}, \\ 60.01\ \text{GeV}^{-2} & \text{HQL}. \end{cases} \quad (54)$$

One can see that there is a small difference between the coupling constants in the exact case, while in the HQL they are practically degenerate. This happens because, as was emphasized before, the coupling constant g_{Λ_Q} in the HQL does not depend on the heavy quark mass. A small difference of the coupling constants g_{Λ_b} and g_{Λ_c} in HQL is due to dependence on $\mathcal{O}(m_Q^0)$ parameters—$\bar{\Lambda}$ and Λ).

The vertex function $\Lambda^\mu_{\Lambda_b\to\Lambda}(p_1, p_2)$ that describes the heavy-to-light $\Lambda_b \to \Lambda$ transition reads

$$\Lambda^\mu_{\Lambda_b\to\Lambda}(p_1,p_2) = 6 g_{\Lambda_b} g_\Lambda \Big\langle\Big\langle \bar{\Phi}_\Lambda(-z_s)\bar{\Phi}_{\Lambda_b}(-z_b) \times S_s(k_1+p_2)\Gamma^\mu S_b(k_1+p_1) \times \text{tr}[S_u(k_2)\gamma^5 S_d(k_2-k_1)\gamma^5]\Big\rangle\Big\rangle, \quad (55)$$

where

$$z_i = \frac{1}{2}(k_1 - k_2 + w_3^i p_2)^2 + \frac{1}{6}(k_1 + k_2 + (2w_2^i + w_3^i)p_2)^2. \quad (56)$$

In the present application we have to consider two cases of Γ^μ: γ^μ and $\gamma^\mu\gamma^5$. The loop calculation contains the variable $v_1 p_2$ that, for a given q^2, is fixed by the kinematics of the process through

$$v_1 p_2 = \frac{m_{\Lambda_b}}{2}\left(1 + \frac{m_\Lambda^2 - q^2}{m_{\Lambda_b}^2}\right), \quad (57)$$

where p_2 and m_Λ are the momentum and mass of the Λ.

In the heavy quark limit we reproduce the form factor structure derived previously from heavy quark effective theory [46–48], which is usually written in the form

$$\bar{u}_2(p_2)\Lambda^\mu_{\Lambda_b\to\Lambda}(p_1,p_2)u_1(p_1) = \bar{u}_2(p_2)[F_1(q^2) + F_2(q^2)\not{v}_1]\Gamma^\mu u_1(p_1). \quad (58)$$

Again, for the present application, Γ^μ is γ^μ or $\gamma^\mu\gamma^5$. From Eq. (58) one finds

$$\begin{aligned} f_1^{V,\rm HQL} &= f_1^{A,\rm HQL} = F_1 + \frac{M_2}{M_1}F_2, \\ f_2^{V,\rm HQL} &= f_2^{A,\rm HQL} = -F_2, \\ f_3^{V,\rm HQL} &= f_3^{A,\rm HQL} = F_2; \end{aligned} \quad (59)$$

i.e. there are only two independent form factors in the HQL. We emphasize that the form factor relations Eq. (59) are valid in the full kinematical region $4m_\ell^2 \le q^2 \le (M_{\Lambda_b} - M_\Lambda)^2$. In Fig. 4 we plot the q^2 dependence of the form factors f_1^V and f_2^V and compare them to the corresponding form factors calculated in the HQL. For the large form factor f_1^V the HQL form factor exceeds the full form factor by $O(10\%)$ while the small form factor f_2^V is lowered by $O(50\%)$.

It is interesting to compare our HQL form factors with the corresponding static lattice results presented in [49]. Although the main concern of [49] was the $\Lambda_b \to p$ form factors, the authors also present results on the $\Lambda_b \to \Lambda$ form factors in their Fig. 4. At $q^2_{\rm max}$, where the lattice calculations are most reliable, one reads off from their Fig. 4 $F_1 = 1.28 \pm 0.05$ and $F_2 = -0.30 \pm 0.02$, where the errors are only statistical, compared to the HQL limiting values $F_1 = 1.21$ and $F_2 = -0.30$ in our model. The agreement is satisfactory. As concerns the q^2 behavior of the form factors our HQL form factors fall off somewhat more steeply than the static lattice form factors. At

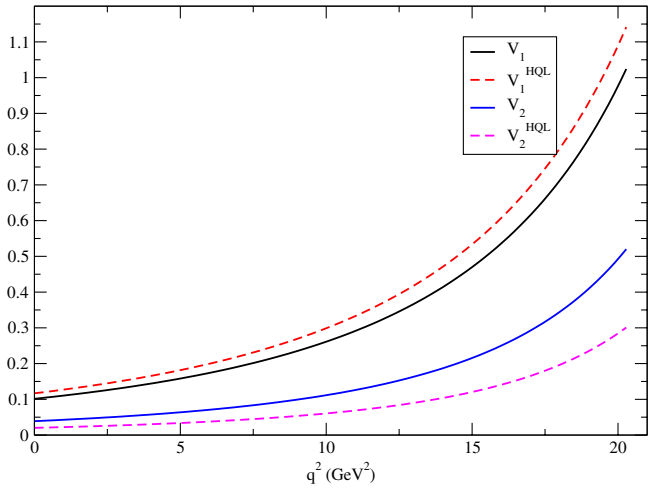

FIG. 4 (color online). Comparison of the form factors $V_i \equiv f_i^V(q^2)$ vs $V_i^{\rm HQL} \equiv f_i^{V,{\rm HQL}}(q^2)$ $(i = 1, 2)$.

$q^2 = 12.4\ {\rm GeV}^2$, where the lattice results may not be so reliable, one finds from Fig. 4 of [49] $F_1 = 0.64 \pm 0.1$ and $F_2 = -0.11 \pm 0.04$, where the errors now include the systematic errors, compared to our values $F_1 = 0.31$ and $F_2 = -0.07$. We mention that the static results given in [49] approximately satisfy the $SU(3)$ relation $F_i(\Lambda_b \to \Lambda) = \sqrt{2/3} F_i(\Lambda_b \to p)$ $(i = 1, 2)$ derived in Eq. (40).

At the large recoil end of the q^2 spectrum soft collinear effective theory predicts that the form factor F_2 vanishes in the heavy quark limit at the leading order of α_s [45,50]. The plot of $f_2^{V,{\rm HQL}}(q^2) = -F_2(q^2)$ in Fig. 4 shows that our prediction for F_2 reaches a very small albeit nonzero value at large recoil.

VI. NUMERICAL RESULTS

We begin by presenting our numerical results for the decay $\Lambda_b \to \Lambda + J/\psi(\to e^+e^-, \mu^+\mu^-)$ for which one can safely use the zero lepton mass approximation (see Table II). Our results are presented in Tables V, VI, and VII where we compare them with the available data [1,11] and predictions of other theoretical approaches [3–10]. In Table V we present our result on the branching fraction $B(\Lambda_b \to \Lambda J/\psi)$ and compare it with data and the results of other theoretical models. The data value of $B(\Lambda_b \to \Lambda J/\psi) = (5.8 \pm 0.8) \times 10^{-4}$ is based on the PDG13 value for $\Gamma(\Lambda_b \to \Lambda J/\psi) \times B(b \to \Lambda_b)$ given in [11] and a value of $B(b \to \Lambda_b) = 0.1$ as used in previous editions of the PDG. Our result on the branching fraction is based on the lifetime measurement 1.429×10^{-12} s as listed in the 2013 update of the PDG [11]. If one would instead take the value of 1.482×10^{-12} s reported in [51], one would have to scale our result on the branching fraction upward by 3.7%. For easy comparison we have taken the freedom to present the results of [9,10] using our parameters (Λ_b life time, CKM matrix elements and Wilson coefficients). Our branching fraction is slightly larger than those of [9,10]. All three branching fractions are somewhat larger than the experimental PDG average value. To judge on the significance of this discrepancy one would have to wait for an absolute measurement of the branching fraction $B(\Lambda_b \to \Lambda J/\psi)$. We mention that the remaining theoretical branching fractions in Table V would have to be readjusted upward by (4–7)% (depending on the year of publication) if the new 2013 lifetime measurement of the LHCb Collaboration [51] is used.

In Table VI we present our result for the asymmetry parameter α_b and compare it with the data and the results of other theoretical models. In agreement with the measurement the theoretical results on the asymmetry parameter come out to be quite small. Since the measurement carries large error bars, one cannot really draw any conclusions on the quality of the agreement between the experiment and the model predictions.

In Table VII we compare our predictions for the asymmetry parameters and the moduli squared of the normalized helicity amplitudes with the corresponding measurements of [1]. The fourth column of Table VII contains our predictions for the corresponding quantities in the decay $\Lambda_b \to \Lambda + \psi(2S)$, which differ notably from the corresponding quantities in the $\Lambda_b \to \Lambda + J/\psi$ mode. The numerical results clearly show the dominance of the $\lambda_\Lambda = -1/2$ helicity configurations in both cases where the dominance is more pronounced for the $\Lambda_b \to \Lambda J/\psi$ mode.

TABLE V. Branching ratio $B(\Lambda_b \to \Lambda + J/\psi)$ (in units of 10^{-4}).

Our result	Theoretical predictions	Data [11]
8.9	2.1 [3]; 1.6 [4]; 2.7 [5]; 6.04 [6]; 2.49 [7]; 3.45 ± 1.81 [8]; 8.4 [9]; 8.2 [10]	5.8 ± 0.8 (PDG average) [11]

TABLE VI. Asymmetry parameter α_b.

Our result	Theoretical predictions	Data [1]
−0.07	−0.11 [3]; −0.10 [4]; −0.21 [5]; −0.18 [6]; −0.208 [7]; −0.155 ± 0.015 [8]; −0.10 [9], −0.09 [10]	−0.04 ± 0.17 ± 0.07

TABLE VII. Asymmetry parameters and moduli squared of normalized helicity amplitudes.

Quantity	Data [1] $\Lambda J/\psi$ mode	Our results $\Lambda J/\psi$ mode	Our results $\Lambda\psi(2S)$ mode
α_b	$-0.04 \pm 0.17 \pm 0.07$	-0.07	0.09
r_0	$0.57 \pm 0.02 \pm 0.01$	0.53	0.45
r_1	$-0.59 \pm 0.10 \pm 0.05$	-0.53	-0.44
$\lvert\hat{H}_{+\frac{1}{2}0}\rvert^2$	$-0.01 \pm 0.04 \pm 0.03$	0.46×10^{-3}	0.33×10^{-2}
$\lvert\hat{H}_{-\frac{1}{2}0}\rvert^2$	$0.58 \pm 0.06 \pm 0.03$	0.53	0.45
$\lvert\hat{H}_{-\frac{1}{2}-1}\rvert^2$	$0.49 \pm 0.05 \pm 0.02$	0.47	0.54
$\lvert\hat{H}_{+\frac{1}{2}+1}\rvert^2$	$-0.06 \pm 0.04 \pm 0.03$	0.31×10^{-2}	0.12×10^{-1}

For the $\Lambda_b \to \Lambda J/\psi$ mode the agreement between our results and the data is quite satisfactory.

Using our results in Table VII we can calculate the three measures Eqs. (26)–(28) characterizing the single angle decay distributions Eqs. (21)–(23). For the polarization related FB asymmetry $A_{\rm FB}|_\theta$ calculated in Eq. (26) one obtains

$$A_{\rm FB}|_\theta = -0.035\, P_b. \tag{60}$$

The analyzing power related to the measurement of the Λ_b-polarization P_b is quite small due to the fact that in our model $|\hat{H}_{+\frac{1}{2}0}|^2 \approx |\hat{H}_{+\frac{1}{2}+1}|^2 \approx 0$ and $|\hat{H}_{-\frac{1}{2}0}|^2 \approx |\hat{H}_{-\frac{1}{2}-1}|^2$ leading to a very small value of the parameter α_b. This is reflected in the poor precision of the polarization measurement $P_b = 0.05 \pm 0.07 \pm 0.02$ reported by the LHCb Collaboration [1].

The second measure $A_{\rm FB}|_{\theta_1}$ related to the hadron-side decay $\Lambda \to p\pi^-$ is nearly maximal in our model due to the fact that the longitudinal polarization of the daughter baryon Λ is close to its maximal value. From Table VII one finds $P_\Lambda^\ell = 2r_1 - \alpha_b = -0,99$ and $P_\Lambda^\ell = -0.97$ for the decays $\Lambda_b \to \Lambda + J/\psi$ and $\Lambda_b \to \Lambda + \psi(2S)$, respectively. For the decay $\Lambda_b \to \Lambda + J/\psi$ the FB asymmetry is given by [see Eq. (27)]

$$A_{\rm FB}|_{\theta_1} = P_\Lambda^\ell \alpha_\Lambda = (2r_1 - \alpha_b)\alpha_\Lambda = -0.64(-0.62), \tag{61}$$

where we have used the experimental value for the asymmetry parameter $\alpha_\Lambda = 0.642$ [11] and where we have added the corresponding number for the $\Lambda_b \to \Lambda\psi(2S)$ mode in round brackets.

Next we discuss the lepton-side $\cos\theta_2$ distribution (23) for the decay $\Lambda_b \to \Lambda V(\to \ell^+\ell^-)$, which is governed by the polarization of the vector charmonium state V. The transverse/longitudinal composition of the vector charmonium state V is given by $\hat{U}$: $\hat{L} = (1 - r_0)$: r_0, where $\hat{U}$ is the sum of the transverse helicity contributions $|\hat{H}_{+\frac{1}{2}+1}|^2 - |\hat{H}_{-\frac{1}{2}-1}|^2$. As mentioned before the electromagnetic decay $V \to \ell^+\ell^-$ is not sensitive to the difference of the two transverse helicity contributions. Table VII shows that the transverse and longitudinal states are approximately equally populated for both vector charmonium states leading to an approximate angular decay distribution of $\hat{W}(\theta_2) \sim \frac{3}{16}(3 - \cos^2\theta_2)$ for $\varepsilon = 0$. The exact numbers are $\hat{U}$: $\hat{L} = 0.47{:}0.53$ and $0.55{:}0.45$ for $V = J/\psi$ and $V = \psi(2S)$, respectively. In Fig. 5 we plot the $\cos\theta$ distribution for the decay $\Lambda_b \to \Lambda J/\psi(\to e^+e^-)$. The convexity of the distribution is characterized by the convexity parameter c_f defined in Eq. (28) for which we obtain $c_f = -0.44$. Negative convexities correspond to a downward open parabola for the decay distribution as is also evident from Fig. 5. Figure 5 also contains a plot of the $\cos\theta_2$ distribution for the case $\Lambda_b \to \Lambda\psi(2S)(\to \tau^+\tau^-)$ for which the convexity parameter is given by $c_f = -0.016$ implying an almost flat $\cos\theta_2$ distribution. Because of the small factor $v^2 = 1 - 4\varepsilon = 0.071$ in the $\cos\theta_2$ distribution Eq. (23)

TABLE VIII. Branching ratios $B(\Lambda_b \to \Lambda + \psi(2S)(\to \ell^+\ell^-))$ in units of 10^{-6}.

Mode	Our results
$\Lambda_b \to \Lambda + e^+e^-$	5.61
$\Lambda_b \to \Lambda + \mu^+\mu^-$	5.61
$\Lambda_b \to \Lambda + \tau^+\tau^-$	2.18

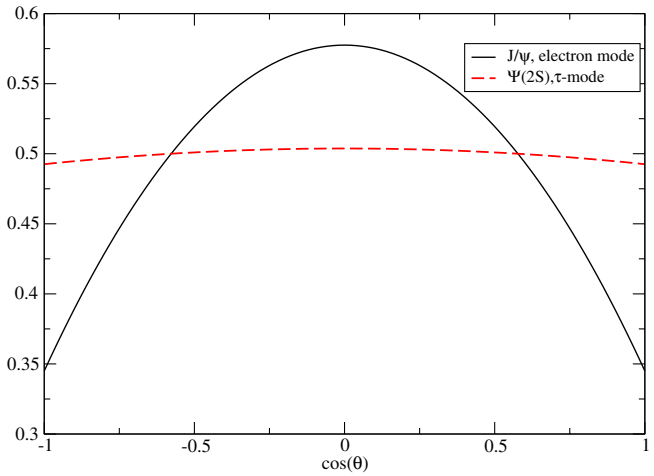

FIG. 5 (color online). Polar angle distribution $\hat{W}(\theta_2)$ for the two cases $\Lambda_b \to \Lambda + J/\psi(\to e^+e^-)$ and $\Lambda_b \to \Lambda + \psi(2S) \times (\to \tau^+\tau^-)$.

the lepton side has lost all of its analyzing power in this case.

As has already been argued after Eq. (29) one expects a minimal azimuthal correlation of the two decay planes spanned by $(p\pi^-)$ and $(\ell^+\ell^-)$. In the zero lepton mass approximation one obtains the azimuthal decay distribution [see Eq. (33)]

$$A_{\rm FB}(\chi) = \frac{\pi}{8\sqrt{2}}\alpha_\Lambda \,{\rm Re}(\hat{H}_{\frac{1}{2}1}\hat{H}^\dagger_{-\frac{1}{2}0} - \hat{H}_{-\frac{1}{2}-1}\hat{H}^\dagger_{\frac{1}{2}0})\cos\chi$$
$$= -0.0046\cos\chi, \qquad (62)$$

where the numerical value can be obtained from the entries in Table VII with the additional information that our model helicity amplitudes (which are real) with helicities $\lambda_\Lambda = -1/2$ and $\lambda_\Lambda = 1/2$ are positive and negative, respectively. As expected, the azimuthal correlation between the two decay planes spanned by $(p\pi^-)$ and $(\ell^+\ell^-)$ is negligibly small. We do not write out the result for the decay $\Lambda_b \to \Lambda + \psi(2S)(\to \tau^+\tau^-)$ since the additional factor of $(1-4\varepsilon)/(1+2\varepsilon) = 0.049$ in (23) reduces the correlation measure to a value close to zero.

Finally, we calculate the cascade $\Lambda_b \to \Lambda + \psi(2S) \times (\to \ell^+\ell^-)$-decay width by using the zero width approximation

$${\rm B}(\Lambda_b \to \Lambda + \psi(2S)(\to \ell^+\ell^-))$$
$$= {\rm B}(\Lambda_b \to \Lambda + \psi(2S))\,{\rm B}(\psi(2S) \to \ell^+\ell^-). \qquad (63)$$

We take the value of the leptonic decay constant $f_{\psi(2S)} = 286.7$ MeV from the electronic mode measured experimentally and employ the formula

$$\Gamma(\psi(2S) \to \ell^+\ell^-)$$
$$= \frac{16\pi\alpha^2}{27}\frac{f^2_{\psi(2S)}}{m_{\psi(2S)}}\sqrt{1-\frac{4m^2_\ell}{m^2_{\psi(2S)}}}\left(1+\frac{2m^2_\ell}{m^2_{\psi(2S)}}\right) \qquad (64)$$

to evaluate the other modes. The results for the branching ratios of the decays $\Lambda_b \to \Lambda + \psi(2S)(\to \ell^+\ell^-)$ are given in Table VIII. Again, one can see that the τ-lepton mass plays an essential role in reducing the value of the decay width as compared to the electron and muon modes. Our prediction for the branching fraction of the $\Lambda_b \to \Lambda + \psi(2S)$ transition is (based on the lifetime value $\tau_{\Lambda_b} = 1.429 \times 10^{-12}$ s)

$$B(\Lambda_b \to \Lambda + \psi(2S)) = 7.25 \times 10^{-4}. \qquad (65)$$

VII. SUMMARY

We have performed a detailed analysis of the decay process $\Lambda_b \to \Lambda + J/\psi$ in the framework of the covariant quark model. We have worked out two variants of threefold joint angular decay distributions in the cascade decay $\Lambda_b \to \Lambda(\to p\pi^-) + J/\psi(\to \ell^+\ell^-)$ for polarized and unpolarized Λ_b decays. We have reported our numerical results on helicity amplitudes, on the rate and on the asymmetry parameters in the decay processes $\Lambda_b \to \Lambda + J/\psi$ and $\Lambda_b \to \Lambda + \psi(2S)$. We have included the decay $\Lambda_b \to \Lambda + \psi(2S)$ in our analysis since this decay allows one to discuss nonzero lepton mass effects in the kinematically allowed decay $\Lambda_b \to \Lambda + \psi(2S)(\to \tau^+\tau^-)$. We confirm expectations from the naive quark model that the transitions into the $\lambda_\Lambda = 1/2$ helicity states of the daughter baryon Λ are strongly suppressed leading to a near maximal negative polarization of the Λ. For the same reason the azimuthal correlation between the two decay planes spanned by $(p\pi^-)$ and $(\ell^+\ell^-)$ is negligibly small. We have compared our results with the available experimental data and with the results of other theoretical approaches. In a separate section we have presented form factor results over the whole accessible range of q^2 values. These results are close to lattice results at minimum recoil and to LCSR results at maximum recoil.

ACKNOWLEDGMENTS

This work was supported by the DFG under Contract No. LY 114/2-1. M. A. I. acknowledges the support from Mainz Institute for Theoretical Physics (MITP) and the Heisenberg-Landau Grant. The work was also partially supported under Project No. 2.3684.2011 of Tomsk State University. This work is also partially supported by the Italian Miur PRIN 2009.

[1] R. Aaij *et al.* (LHCb Collaboration), Phys. Lett. B **724**, 27 (2013).
[2] A. K. Leibovich, Z. Ligeti, I. W. Stewart, and M. B. Wise, Phys. Lett. B **586**, 337 (2004).
[3] H.-Y. Cheng and B. Tseng, Phys. Rev. D **53**, 1457 (1996); **55**, 1697(E) (1997).
[4] H.-Y. Cheng, Phys. Rev. D **56**, 2799 (1997).
[5] M. A. Ivanov, J. G. Körner, V. E. Lyubovitskij, and A. G. Rusetsky, Phys. Rev. D **57**, 5632 (1998).
[6] Fayyazuddin and Riazuddin, Phys. Rev. D **58**, 014016 (1998).
[7] R. Mohanta, A. K. Giri, M. P. Khanna, M. Ishida, S. Ishida, and M. Oda, Prog. Theor. Phys. **101**, 959 (1999).
[8] C.-H. Chou, H.-H. Shih, S.-C. Lee, and H.-n. Li, Phys. Rev. D **65**, 074030 (2002).
[9] Z.-T. Wei, H.-W. Ke, and X.-Q. Li, Phys. Rev. D **80**, 094016 (2009).

[10] L. Mott and W. Roberts, Int. J. Mod. Phys. A **27**, 1250016 (2012).

[11] J. Beringer *et al.* (Particle Data Group), Phys. Rev. D **86**, 010001 (2012); and 2013 partial update for the 2014 edition.

[12] F. Abe *et al.* (CDF Collaboration), Phys. Rev. D **55**, 1142 (1997).

[13] V. M. Abazov *et al.* (D0 Collaboration), Phys. Rev. D **84**, 031102 (2011).

[14] M. A. Ivanov, M. P. Locher, and V. E. Lyubovitskij, Few-Body Syst. **21**, 131 (1996).

[15] M. A. Ivanov, V. E. Lyubovitskij, J. G. Körner, and P. Kroll, Phys. Rev. D **56**, 348 (1997).

[16] M. A. Ivanov, J. G. Körner, and V. E. Lyubovitskij, Phys. Lett. B **448**, 143 (1999).

[17] M. A. Ivanov, J. G. Körner, V. E. Lyubovitskij, and A. G. Rusetsky, Phys. Rev. D **60**, 094002 (1999).

[18] M. A. Ivanov, J. G. Körner, V. E. Lyubovitskij, M. A. Pisarev, and A. G. Rusetsky, Phys. Rev. D **61**, 114010 (2000).

[19] M. A. Ivanov, J. G. Körner, V. E. Lyubovitskij, and A. G. Rusetsky, Phys. Lett. B **476**, 58 (2000).

[20] A. Faessler, T. Gutsche, M. A. Ivanov, J. G. Körner, and V. E. Lyubovitskij, Phys. Lett. B **518**, 55 (2001).

[21] A. Faessler, T. Gutsche, M. A. Ivanov, J. G. Körner, and V. E. Lyubovitskij, Eur. Phys. J. direct C **4**, 1 (2002).

[22] A. Faessler, T. Gutsche, M. A. Ivanov, J. G. Körner, V. E. Lyubovitskij, D. Nicmorus, and K. Pumsa-ard, Phys. Rev. D **73**, 094013 (2006).

[23] A. Faessler, T. Gutsche, B. R. Holstein, M. A. Ivanov, J. G. Körner, and V. E. Lyubovitskij, Phys. Rev. D **78**, 094005 (2008).

[24] A. Faessler, T. Gutsche, M. A. Ivanov, J. G. Körner, and V. E. Lyubovitskij, Phys. Rev. D **80**, 034025 (2009).

[25] T. Branz, A. Faessler, T. Gutsche, M. A. Ivanov, J. G. Körner, V. E. Lyubovitskij, and B. Oexl, Phys. Rev. D **81**, 114036 (2010).

[26] S. Dubnicka, A. Z. Dubnickova, M. A. Ivanov, and J. G. Körner, Phys. Rev. D **81**, 114007 (2010).

[27] S. Dubnicka, A. Z. Dubnickova, M. A. Ivanov, J. G. Körner, P. Santorelli, and G. G. Saidullaeva, Phys. Rev. D **84**, 014006 (2011).

[28] T. Branz, A. Faessler, T. Gutsche, M. A. Ivanov, J. G. Körner, and V. E. Lyubovitskij, Phys. Rev. D **81**, 034010 (2010).

[29] M. A. Ivanov, J. G. Körner, S. G. Kovalenko, P. Santorelli, and G. G. Saidullaeva, Phys. Rev. D **85**, 034004 (2012).

[30] S. Dubnicka, A. Z. Dubnickova, M. A. Ivanov, and A. Liptaj, Phys. Rev. D **87**, 074201 (2013).

[31] T. Gutsche, M. A. Ivanov, J. G. Körner, V. E. Lyubovitskij, and P. Santorelli, Phys. Rev. D **86**, 074013 (2012).

[32] T. Gutsche, M. A. Ivanov, J. G. Körner, V. E. Lyubovitskij, and P. Santorelli, Phys. Rev. D **87**, 074031 (2013).

[33] W. Altmannshofer, P. Ball, A. Bharucha, A. J. Buras, D. M. Straub, and M. Wick, J. High Energy Phys. 01 (2009) 019.

[34] A. Kadeer, J. G. Körner, and U. Moosbrugger, Eur. Phys. J. C **59**, 27 (2009).

[35] R. Lednicky, Sov. J. Nucl. Phys. **43**, 817 (1986).

[36] P. Bialas, J. G. Körner, M. Krämer, and K. Zalewski, Z. Phys. C **57**, 115 (1993).

[37] J. Hrivnac, R. Lednicky, and M. Smizanska, J. Phys. G **21**, 629 (1995).

[38] S. Weinberg, Phys. Rev. **130**, 776 (1963).

[39] A. Salam, Nuovo Cimento **25**, 224 (1962).

[40] K. Hayashi, M. Hirayama, T. Muta, N. Seto, and T. Shirafuji, Fortschr. Phys. **15**, 625 (1967).

[41] G. V. Efimov and M. A. Ivanov, *The Quark Confinement Model of Hadrons* (IOP Publishing, Bristol, 1993).

[42] J. A. M. Vermaseren, Nucl. Phys. B, Proc. Suppl. **183**, 19 (2008); arXiv:math-ph/0010025.

[43] A. Khodjamirian, C. Klein, T. Mannel, and Y.-M. Wang, J. High Energy Phys. 09 (2011) 106.

[44] T. A. Kaeding, arXiv:nucl-th/9502037.

[45] T. Mannel and Y.-M. Wang, J. High Energy Phys. 12 (2011) 067.

[46] F. Hussain, J. G. Körner, M. Krämer, and G. Thompson, Z. Phys. C **51**, 321 (1991).

[47] F. Hussain, D.-S. Liu, M. Krämer, J. G. Körner, and S. Tawfiq, Nucl. Phys. **B370**, 259 (1992).

[48] T. Mannel, W. Roberts, and Z. Ryzak, Nucl. Phys. **B355**, 38 (1991).

[49] W. Detmold, C.-J. D. Lin, S. Meinel, and M. Wingate, Phys. Rev. D **88**, 014512 (2013).

[50] T. Feldmann and M. W. Y. Yip, Phys. Rev. D **85**, 014035 (2012); **86**, 079901(E) (2012).

[51] R. Aaij *et al.* (LHCb Collaboration), Phys. Rev. Lett. **111**, 102003 (2013).